



Received 16 May 2017
Accepted 20 May 2017

Edited by M. Zeller, Purdue University, USA

Keywords: crystal structure; acrylamide; benzotriazole; benzotriazolylpropanamide; hydrogen bond; π - π stacking.

CCDC references: 1550158; 1550157;
1550156

Supporting information: this article has supporting information at journals.iucr.org/e

Synthesis and crystal structures of three new benzotriazolylpropanamides

Donna S. Amenta,^a Phil Liebing,^b Julia E. Biero,^a Robert J. Sherman,^a John W. Gilje^{a*} and Frank T. Edelmann^{b*}

^aChemistry Department, James Madison University, Harrisonburg, VA 22807, USA, and ^bChemisches Institut der Otto-von-Guericke-Universität Magdeburg, Universitätsplatz 2, 39106 Magdeburg, Germany. *Correspondence e-mail: giljejw@jmu.edu, frank.edelmann@ovgu.de

The base-catalyzed Michael addition of 2-methylacrylamide to benzotriazole afforded 3-(1*H*-benzotriazol-1-yl)-2-methylpropanamide, C₁₀H₁₂N₄O (**1**), in 32% yield in addition to small amounts of isomeric 3-(2*H*-benzotriazol-2-yl)-2-methylpropanamide, C₁₀H₁₂N₄O (**2**). In a similar manner, 3-(1*H*-benzotriazol-1-yl)-*N,N*-dimethylpropanamide, C₁₁H₁₄N₄O (**3**), was prepared from benzotriazole and *N,N*-dimethylacrylamide. All three products have been structurally characterized by single-crystal X-ray diffraction. The crystal structures of **1** and **2** comprise infinite arrays formed by N—H···O and N—H···N bridges, as well as π — π interactions, while the molecules of **3** are aggregated to simple π -dimers in the crystal.

1. Chemical context

Di- and tridentate pyrazolyl-based ligands play an important role in the design of supramolecular assemblies of metal complexes. Particularly notable among the large variety of such ligands are Trofimenko's famous poly(pyrazolyl)borates ('scorpionates') (Trofimenko, 1993, 2004; Marques *et al.*, 2002; Paulo *et al.*, 2004; Smith, 2008) and the poly(pyrazolyl)-methane ligands (Bassanetti *et al.*, 2016; Bigmore *et al.*, 2005; Kriek *et al.*, 2016; Otero *et al.*, 2013; Semeniuc & Reger, 2016). In a series of previous studies, we reported the synthesis and supramolecular coordination chemistry of the simple, functionalized pyrazolyl-based ligand 3-(pyrazol-1-yl)propanamide. This ligand is readily available in one step *via* base-catalyzed Michael addition of pyrazole to acrylamide (Girma *et al.*, 2008). In combination with various first- and second-row transition metals (*e.g.* Mn, Fe, Ru, Co, Ni), 3-(1*H*-pyrazol-1-yl)propanamide allows the design of a variety of hydrogen-

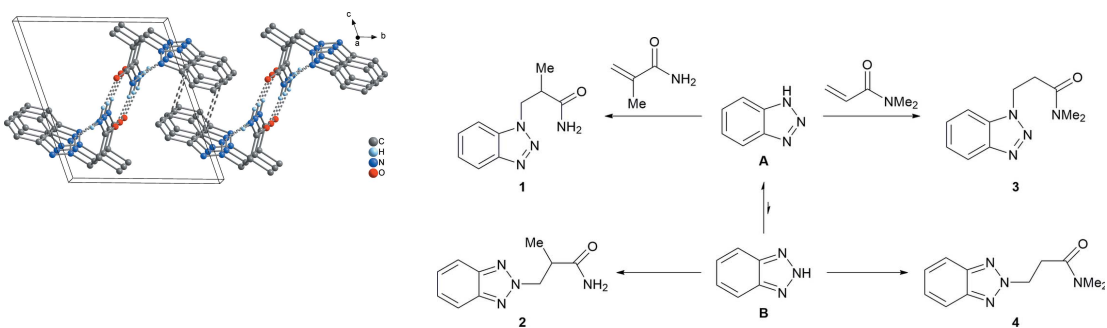


Figure 1

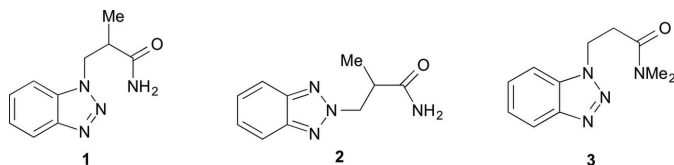
Formation of the 1*H*- and 2*H*-benzotriazolylpropanamides **1–4** from benzotriazole.

OPEN ACCESS

bonded supramolecular assemblies, including different chains, sheets, and three-dimensional arrays (D'Amico *et al.*, 2015). As an additional advantage, the pyrazolylpropanamide ligand system can be easily modified either by attachment of substituents to the propanamide backbone (D'Amico *et al.*, 2015) or by replacing the pyrazole ring by other *N*-heterocycles such as triazole (D'Amico *et al.*, 2015; Wagner *et al.*, 2012). In our most recent study, we investigated the structural influence of benzotriazolyl as a hydrophobic functional group, which imparts amphiphilic character to the ligand and forms the basis of novel supramolecular assemblies. In the course of this work, the solid-state structures of 3-(1*H*-benzotriazol-1-yl)-propaneamide (= 'BTPA') and of several first-row transition metal complexes (Mn, Co, Cu) derived thereof have been described (Wang *et al.*, 2017). We report here the synthesis and structural characterization of three new potentially useful benzotriazolylpropanamide ligands.

The title compounds were prepared by base-catalyzed Michael addition of benzotriazole to methyl-substituted acrylamides, namely 2-methylacrylamide and *N,N*-dimethylacrylamide. As shown in the reaction scheme (Fig. 1), benzotriazole exists in two tautomeric forms **A** and **B**. Spectroscopic data (UV, IR and ¹H NMR) (Negri & Caminati, 1996; Nesmeyanov *et al.*, 1969; Poznański *et al.*, 2007) and dipole moment measurements (Mauret *et al.*, 1974) revealed that the 1*H*-tautomer **A** is the predominant species at room temperature.

The thermal reaction of benzotriazole with 2-methylacrylamide was carried out in the usual manner (D'Amico *et al.*, 2015; Wagner *et al.*, 2012; Wang *et al.*, 2017) in the presence of Triton B (= benzyltrimethylammonium hydroxide) as basic catalyst. Repeated recrystallization of the crude product from ethanol afforded 3-(1*H*-benzotriazol-1-yl)-2-methylpropanamide (**1**) in 32% isolated yield. The compound was characterized through elemental analysis as well as IR and NMR (¹H, ¹³C) spectroscopy. In the ¹³C NMR spectrum, the amide carbonyl C atom gives a characteristic resonance at 175.2 ppm. The formation of **1** as the main reaction product corresponds to the predominant presence of tautomer **A** in the starting benzotriazole. From the mother liquor of the recrystallization of **1**, a small amount of colorless crystals could be isolated, which were found to be the isomer 3-(2*H*-benzotriazol-2-yl)-2-methylpropanamide (**2**) resulting from the reaction of the 2*H*-tautomer **B** with 2-methylacrylamide. Compound **2** could also be fully characterized by elemental analysis as well as IR and NMR data.



In a similar manner, a reaction of benzotriazole with neat *N,N*-dimethylacrylamide in the presence of Triton B afforded a yellow oil which was shown to be an approximate 2:1 mixture of **3** and **4**. Once again, the main component was the Michael addition product resulting from the 1*H*-tautomer **A** of

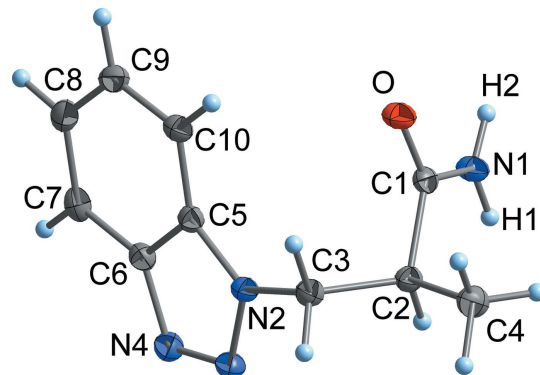


Figure 2

The molecular structure of **1** in the crystal. Displacement ellipsoids are drawn at the 50% probability level.

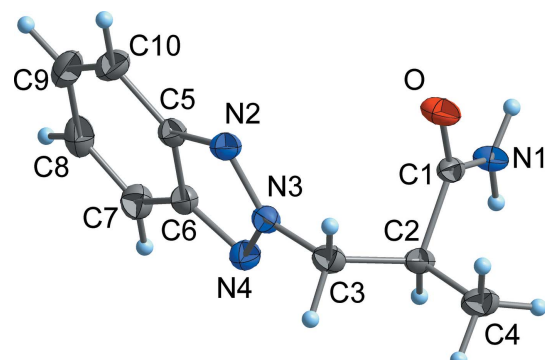


Figure 3

The molecular structure of **2** in the crystal. Displacement ellipsoids are drawn at the 50% probability level.

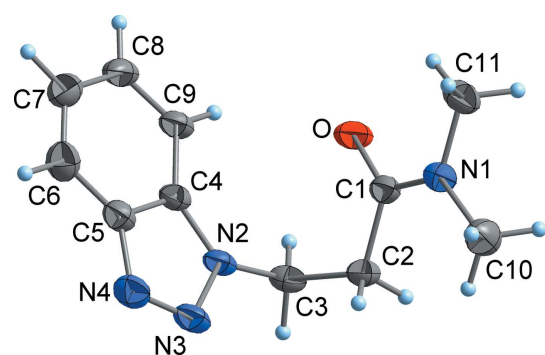


Figure 4

The molecular structure of **3** in the crystal. Displacement ellipsoids are drawn at the 50% probability level. The methyl group C11 shows rotational disorder over two orientations (only one orientation of the H atoms is shown).

benzotriazole. Thus far, only isomer **3** could be isolated in pure form by recrystallization of the oily crude product from ethanol. The identity of 3-(1*H*-benzotriazol-1-yl)-*N,N*-dimethylpropanamide **3** was confirmed by elemental analysis and spectroscopic data (IR, ¹H and ¹³C NMR). In the ¹³C NMR spectrum, the NMe₂ group gives rise to two resonances at δ 33.2 and 35.5 ppm, whereas the signal of the amide carbonyl C atom is found at δ 169.5 ppm.

Table 1Hydrogen-bond geometry (\AA , $^\circ$) for **1**.

$D-\text{H}\cdots A$	$D-\text{H}$	$\text{H}\cdots A$	$D\cdots A$	$D-\text{H}\cdots A$
N1—H2 \cdots O ⁱ	0.88	2.02	2.8970 (12)	175
N1—H1 \cdots N4 ⁱⁱ	0.88	2.16	3.0017 (14)	161

Symmetry codes: (i) $-x, -y + 1, -z + 2$; (ii) $-x, -y + 2, -z + 1$.**Table 2**Hydrogen-bond geometry (\AA , $^\circ$) for **2**.

$D-\text{H}\cdots A$	$D-\text{H}$	$\text{H}\cdots A$	$D\cdots A$	$D-\text{H}\cdots A$
N1—H1 \cdots O ⁱ	0.88	2.00	2.8745 (18)	170
N1—H2 \cdots N2 ⁱⁱ	0.88	2.24	3.0850 (18)	161

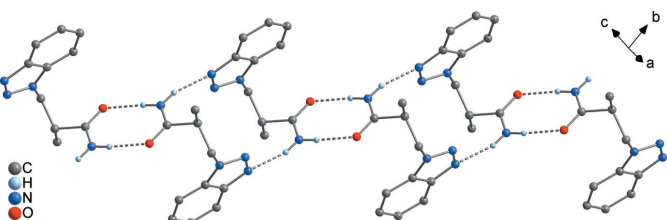
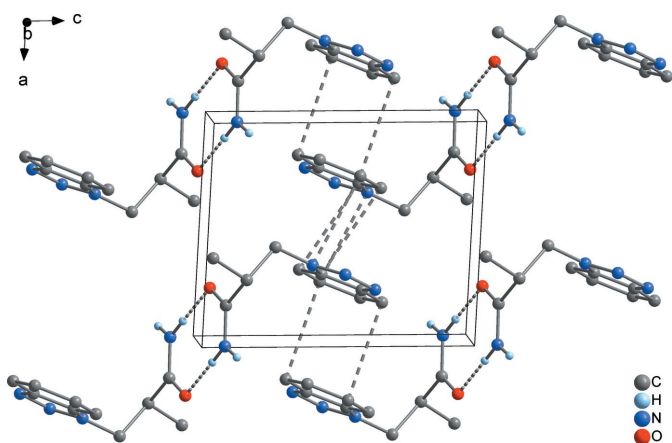
Symmetry codes: (i) $-x, -y + 1, -z + 1$; (ii) $x - 1, y, z$.

2. Structural commentary

Compounds **1–3** exist as well-defined monomeric molecules in the crystal, without any solvent of crystallization (Figs. 2–4). The C=O separations are in a narrow range around 1.24 \AA and are therefore virtually equal with those observed in related functionalized propanamides (Girma *et al.* 2008; Wagner *et al.* 2012; D'Amico *et al.* 2015; Wang *et al.* 2017). Thus, the C=O distance is not markedly influenced by hydrogen bonding, as there are N—H \cdots O bridges in **1** and **2**, but not in **3** (see *Supramolecular features* section). The same applies to the amide C—N separation, which is around 1.33 \AA in all compounds. The torsion angle C1—C2—C3—N between the amide group and the 1*H*-benzotriazol-1-yl residue is 71.0 (1) $^\circ$ (**1**) and -72.2 (2) $^\circ$ (**3**), respectively, which is close to the value observed in the unsubstituted BTPA (71.3 (1) $^\circ$; Wang *et al.*, 2017). By contrast, the same torsion angle in the 2*H*-benzotriazole-derived compound **2** is considerably smaller at 59.7 (1) $^\circ$.

3. Supramolecular features

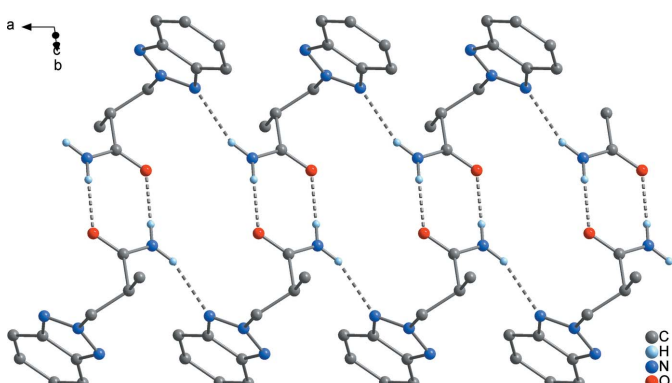
In **1** and **2**, the molecules are interconnected to dimeric subunits by $R_2^2(8)$ -type N—H \cdots O bridges, which is a very typical motif (Bernstein *et al.*, 1995). These amide dimers are again interconnected by N—H \cdots N bridges (Tables 1 and 2) between the remaining amide N—H moiety and the benzotriazolyl group, resulting in an infinite chain of rings in both cases. In **1**, the dimeric subunits are linked by a $R_2^2(16)$ bridge

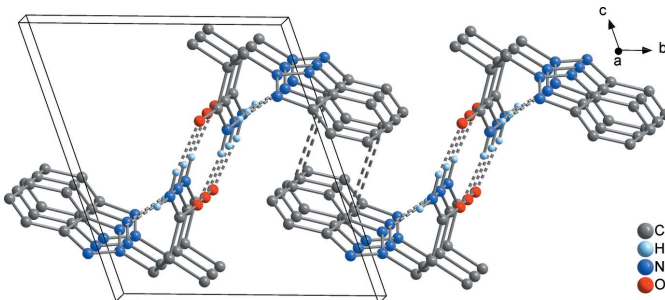
**Figure 5**Supramolecular chain of rings in **1**, formed by N—H \cdots O and N—H \cdots N bridging.**Figure 6**

The unit cell of **1**, illustrating the aggregation of the chains shown in Fig. 5 by π \cdots π stacking into a three-dimensional framework, viewed in a projection on (010).

to N4 (Fig. 5), while a C(7) bridge involving N2 is realized in compound **2** (Fig. 7). The latter leads to an $R_4^4(18)$ motif at the binary level. The hydrogen-bridge pattern in **1** and **2** is therefore entirely different than in the unbridged BTPA, where supramolecular layers are formed exclusively by N—H \cdots O bridges (Wang *et al.*, 2017). As has been discussed for BTPA and its metal complexes, the N—H \cdots N bonds are significantly weaker than the N—H \cdots O bonds. Both the N \cdots O separation [**1**: N1 \cdots O 2.897 (1) \AA ; **2**: N1 \cdots O 2.875 (2) \AA] and the N \cdots N separations [**1**: N1 \cdots N4 3.002 (1) \AA ; **2**: N1 \cdots N2 3.085 (2) \AA] are in the typical range. In the crystal structure of **3**, no hydrogen bonds are present as the amide H atoms are replaced by methyl groups.

In both **1** and **2**, the supramolecular chains are further aggregated by π \cdots π interactions between the benzotriazolyl rings. In **1**, a three-dimensional framework is present (Fig. 6), where two different types of π interactions can be distinguished. First, the C₆ rings of each two adjoining benzotriazolyl groups are stacked in a typical parallel-displaced fashion (cf. Fig. 10a). The shortest C \cdots C contact is 3.364 (2) \AA between C7 and C9 and the distance between the C₆ ring

**Figure 7**Supramolecular chain of rings in **2**, formed by N—H \cdots O and N—H \cdots N bridging, extending along the crystallographic *a* axis.

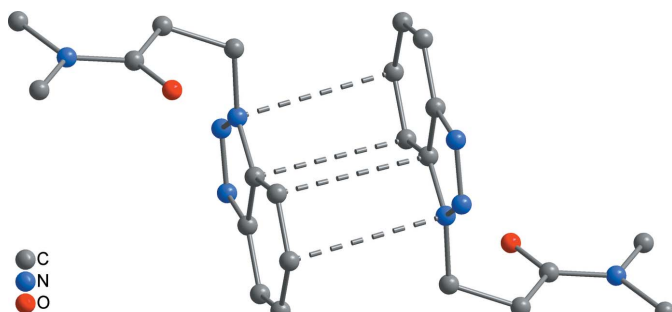
**Figure 8**

The unit cell of **2**, illustrating the aggregation of the chains shown in Fig. 6 by π - π stacking, to a two-dimensional array extending parallel to (001), viewed in a projection on (100).

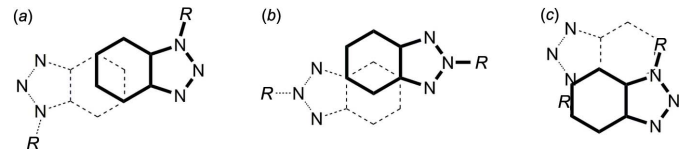
centroids is 3.655 (2) Å, which is in the range of strong π interactions (McGaughey *et al.*, 1998). The so-formed π dimers are interconnected by another π interaction to an infinite chain, where an attractive interaction seems to exist between the whole bicyclic C_6N_3 system rather than between the C_6 rings only (*cf.* Fig. 10*c*). The closest intermolecular separations are 3.308 (2) Å (C9···N2) and 3.403 (2) Å (C5···C10), and therefore in the same range as in the former mentioned interaction. In the case of **2**, a layer structure parallel to (001) is formed (Fig. 8). The geometry of the interaction between the C_6 rings is similar as in **1**, but the closest C···C contact exists between C5 and C9 with 3.521 (2) Å, and the corresponding separation between the C_6 centroids is considerably larger at 3.933 (2) Å (*cf.* Fig. 10*b*). In **3**, only two molecules are stacked together to a simple π dimer (Fig. 9), with participation of the whole C_6N_3 bicycle similar as described above for **1** (*cf.* Fig. 10*c*). Here, the closest intermolecular contacts are 3.468 (2) Å (C8···N2) and 3.509 (2) Å (C4···C9), which is significantly larger than in **1**. Comparable π interactions as in **1–3** have not been observed in the unbridged BTPA, but in its metal complexes $[MCl_2(BTPA)_2]$ ($M = Mn, Co, Cu$; min. C···C 3.45 Å; Wang *et al.*, 2017). The arrangement of the benzotriazolyl groups in the latter compounds is similar to that in **3** (*cf.* Fig. 10*c*).

4. Database survey

For reviews on di- and tridentate pyrazolyl-based ligands, see Bassanetti *et al.* (2016), Bigmore *et al.* (2005), Krieck *et al.*

**Figure 9**

Supramolecular dimer of **3**, formed by π - π stacking.

**Figure 10**

Comparison of the arrangement of the benzotriazolyl rings in the crystal structures of 3-benzotriazolylpropanamides: stacking of C_6 rings in **1** (*a*) and in **2** (*b*), stacking of C_6N_3 bicycles in **1**, **3** and in $[MCl_2(BTPA)_2]$ ($M = Mn, Co, Cu$) (*c*), each viewed in a projection on the C_6N_3 plane.

(2016), Marques *et al.* (2002), Otero *et al.* (2013), Paulo *et al.* (2004), Semeniuc & Reger (2016), Smith (2008), Trofimenko (1993, 2004).

For the tautomerism of benzotriazole, see Mauret *et al.* (1974), Negri & Caminati (1996); Nesmeyanov *et al.* (1969), Poznański *et al.* (2007).

For other structurally characterized 3-pyrazolylpropanamide-derived ligands, see D'Amico *et al.* (2015), Girma *et al.* (2008), Wagner *et al.* (2012), Wang *et al.* (2017).

5. Synthesis and crystallization

All manipulations were performed under inert nitrogen or argon atmospheres using standard Schlenk techniques or in a Vacuum Atmospheres Glove Box. The starting materials were obtained from commercial sources and used as received. Solvents were dried using an Innovative Technology, Inc, solvent purification system. Microanalysis was performed by Galbraith Laboratories, Inc, Knoxville, TN, USA. NMR spectra were obtained using Bruker Avance 300 MHz and 400 MHz NMR Spectrometers. IR spectra were recorded using KBr pellets with a ThermoNicolet Avatar 370 FT-IR between 4000 cm⁻¹ and 400 cm⁻¹.

*Preparation of 2-methyl-3-(1H-benzotriazol-1-yl)propanamide (**1**) and 2-methyl-3-(2H-benzotriazol-2-yl)propanamide (**2**):*

In a 150 mL three-neck flask, a mixture of benzotriazole (5.032 g, 42.24 mmol), 2-methyl acrylamide (3.731 g, 43.84 mmol) and 2 mL of Triton B was heated for 6.5 h in a boiling water bath. The mixture solidified upon cooling. The crude product was slurried with 95% ethanol and the remaining solid recrystallized three times from 95% ethanol to yield 2.841 g (13.91 mmol, 32%) of spectroscopically pure **1**. Single crystals suitable for X-ray diffraction were obtained from these recrystallizations. M.p. 476–479 K. Analysis calculated for $C_{10}H_{12}N_4O$, $M = 204.20$ g mol⁻¹: C 58.82; H 5.92; N 27.44. Found: C 58.73; H 5.96; N 27.72. IR (KBr, cm⁻¹): 3307 vs, 3208 s, 3155 vs, 2968 m, 2930 w, 1685 vs, 1442 m, 1315 m, 1226 s, 780 m, 742 vs. ¹H NMR (400 MHz, DMSO-*d*₆): 1.07 (d, *J*₂₋₄ = 7 Hz, 3H; *CH*₃), 3.06 (sext, *J*₂₋₄ = 7 Hz, *J*₂₋₃ = 7 Hz, 1H; 2-CH), 4.61 (dd, *J*₂₋₃ = 7 Hz, *J*_{2-2'} = 14 Hz, 1H; *CH*₂), 4.86 (dd, *J*₂₋₃ = 7 Hz, *J*_{2-2'} = 14 Hz, 1H; *CH*₂), 6.88 (s br, 1H; NH), 7.39 (m, 1H; 8-CH or 9-CH), 7.42 (s br, 1H; NH) 7.54 (m, 1H; 8-CH or 9-CH), 7.87 (m, 1H; 7-CH or 10-CH), 8.02 (m, 1H; 7-CH or 10-CH) ppm. The resonances for positions 7–10 appear as multiplets that can be interpreted if the coupling constants

Table 3
Experimental details.

	1	2	3
Crystal data			
Chemical formula	$C_{10}H_{12}N_4O$	$C_{10}H_{12}N_4O$	$C_{11}H_{14}N_4O$
M_r	204.24	204.24	218.26
Crystal system, space group	Triclinic, $P\bar{1}$	Triclinic, $P\bar{1}$	Triclinic, $P\bar{1}$
Temperature (K)	100	133	153
a, b, c (Å)	7.3885 (9), 8.072 (1), 9.2976 (13)	5.5961 (11), 9.3462 (19), 10.472 (2)	7.1732 (6), 7.9945 (6), 9.5912 (7)
α, β, γ (°)	69.039 (12), 89.498 (10), 75.915 (10)	109.83 (3), 90.93 (3), 97.14 (3)	83.910 (6), 86.247 (6), 81.528 (6)
V (Å ³)	500.37 (12)	510.2 (2)	540.25 (7)
Z	2	2	2
Radiation type	Cu $K\alpha$	Mo $K\alpha$	Mo $K\alpha$
μ (mm ⁻¹)	0.76	0.09	0.09
Crystal size (mm)	0.15 × 0.10 × 0.08	0.48 × 0.33 × 0.25	0.34 × 0.32 × 0.28
Data collection			
Diffractometer	Agilent Xcalibur, Atlas, Nova	Stoe IPDS 2T	Stoe IPDS 2T
Absorption correction	Multi-scan (<i>CrysAlis PRO</i> , Agilent, 2003)	–	–
T_{min}, T_{max}	0.919, 1.000	–	–
No. of measured, independent and observed [$I > 2\sigma(I)$] reflections	28193, 2053, 2012	3731, 1774, 1653	4194, 1904, 1596
R_{int}	0.026	0.056	0.062
(sin θ/λ) _{max} (Å ⁻¹)	0.626	0.595	0.595
Refinement			
$R[F^2 > 2\sigma(F^2)], wR(F^2), S$	0.032, 0.081, 1.11	0.037, 0.087, 1.09	0.047, 0.131, 1.03
No. of reflections	2053	1774	1904
No. of parameters	138	138	149
H-atom treatment	H-atom parameters constrained	H-atom parameters constrained	H-atom parameters constrained
$\Delta\rho_{max}, \Delta\rho_{min}$ (e Å ⁻³)	0.33, -0.21	0.25, -0.18	0.22, -0.20

Computer programs: *CrysAlis PRO* (Agilent, 2003), *X-AREA* and *X-RED* (Stoe & Cie, 2002), *SHELXS97* (Sheldrick, 2008), *SIR97* (Altomare *et al.*, 1999), *SHELXL2016* (Sheldrick, 2015) and *DIAMOND* (Brandenburg, 1999).

between adjacent protons are 7–8 Hz, with longer range couplings of about 1 Hz. ¹³C{¹H} NMR (100 MHz, DMSO-*d*₆): 16.2 (CH₃), 40.6 (2-CH), 50.6 (CH₂), 111.5 (10-CH), 119.4 (7-CH), 124.3 (8-CH), 127.5 (9-CH), 133.5 (5-C), 145.4 (6-C), 175.3 (CO) (for numbering scheme *cf.* Fig. 2).

The mother liquor remaining after the isolation of **1** was concentrated, and two additional crops of crystals were obtained. The second crop was several milligrams of nearly pure **2** and contained crystals suitable for X-ray diffraction. M.p. 476–479 K. Analysis calculated for $C_{10}H_{12}N_4O$, $M = 204.20$ g mol⁻¹: C 58.82; H 5.92; N 27.44. Found: C 58.92; H 6.20; N 27.50. IR (KBr, cm⁻¹): 3307 vs, 3208 s, 3155 vs, 2968 *m*, 2930 *w*, 1685 vs, 1442 *m*, 1315 *m*, 1226 *s*, 780 *m*, 742 vs. ¹H NMR (400 MHz, DMSO-*d*₆): 1.06 (*d*, $J_{2-4} = 7.0$ Hz, 3H; CH₃), 3.06 (*sext*, $J_{2-4} = 7.0$ Hz, $J_{2-3} = 7.0$ Hz, $J_{2-3'} = 7.7$ Hz, 1H; 2-CH), 4.64 (*dd*, $J_{2-3} = 7.0$ Hz, $J_{3-3'} = 13.3$ Hz, 1H; CH₂), 4.93 (*dd*, $J_{2-3} = 7.7$ Hz, $J_{3-3'} = 13.3$ Hz, 1H; CH₂), 6.91 (*s br*, 1H; NH), 7.43 (*m*, 2H; 6,9-CH), 7.48 (*s br*; NH), 7.91 (*m*, 2H; 7,8-CH). The resonances for 6-CH, 7-CH, 8-CH and 9-CH appear as an AA'BB' pattern. While there is no unique solution for AA'BB' spectra, the ¹H spectrum of the aromatic region of **2** can be duplicated using reasonable values of the coupling constants: $J_{7-8} = 6.8$ Hz, $J_{6-7} = J_{8-9} = 8.6$ Hz, $J_{6-8} = J_{7-9} = 1.0$ Hz, and $J_{6-9} = 1.0$ Hz. ¹³C{¹H} NMR (100 MHz, DMSO-*d*₆): 16.2 (CH₃), 40.5 (2-CH), 58.5 (CH₂), 118.3 (6,9-CH), 126.8 (7,8-CH), 144.1 (5,10-C), 175.0 (CO) (for numbering scheme *cf.* Fig. 3).

Preparation of *N,N*-dimethyl-3-(1*H*-benzotriazol-1-yl)propanamide (**3**):

In a 150 mL three-neck flask, a mixture of benzotriazole (5.99 g, 50.0 mmol), *N,N*-dimethylacrylamide (4.78 g, 48.8 mmol) and 2 mL of Triton B was heated for 6.5 h in a boiling water bath under nitrogen. Upon cooling to 278 K, a yellow oil was obtained. This mixture was an approximate 2:1 mixture of **3** and **4**. After recrystallization from ethanol, samples of pure **3** could be obtained. Single crystals suitable for X-ray diffraction were obtained from recrystallization from a CHCl₃/hexanes mixture. M.p. 338–339 K. Analysis calculated for $C_{10}H_{12}N_4O$, $M = 218.26$ g mol⁻¹: C 60.53; H 6.47; N 25.60. Found: C 60.48; H 6.27; N 25.87. IR (KBr, cm⁻¹): 3082 *w*, 3050 *w*, 3015 *w*, 2967 *m*, 2939 *m*, 2911 *m*, 1644 vs, 1496 *s*, 1452 *s*, 1414 *s*, 1396 *s*, 1338 *m*, 1298 *m*, 1216 *s*, 1151 *s*, 1092 *s*, 942 *m*, 761 *s*, 743 vs. ¹H NMR (300 MHz, CDCl₃): 2.92 (*s*, 3H; NCH₃), 2.94 (*s*; NCH₃), 3.14 (*t*, $J_{2-3} = 7$ Hz, 2H; 2-CH₂), 4.98 (*t*, $J_{2-3} = 7$ Hz, 2H; 3-CH₂), 7.38 (*m*, 2H; 7-CH or 8-CH), 7.51 (*m*, 2H; 7-CH or 8-CH), 7.20 (*m*, 2H; 6-CH or 9-CH), 8.05 (*m*, 2H; 6-CH or 9-CH). The resonances for positions 6–9 appear as multiplets that can be interpreted if the coupling constants between adjacent protons are 7–8 Hz, with longer range couplings of about 1 Hz. ¹³C{¹H} NMR (100 MHz, CDCl₃): 33.2 (NCH₃), 35.5 (NCH₃), 37.0 (2-CH₂), 43.9 (3-CH₂), 110.0 (9-CH), 119.7 (6-CH), 123.9 (7-CH), 127.4 (8-CH), 133.3 (4-C), 145.8 (5-C), 169.5 (CO) (for numbering scheme *cf.* Fig. 4).

6. Refinement

Crystal data, data collection and structure refinement details are summarized in Table 3. All H atoms were fixed geometrically using a riding model with $U_{\text{iso}}(\text{H}) = 1.2 U_{\text{eq}}(X)$ ($X = \text{C}, \text{N}$). The CH_3 groups were allowed to rotate freely around the $\text{C}-X$ vector ($X = \text{C}, \text{N}$) (AFIX 137 in SHELXL), and the amide NH_2 groups in **1** and **2** were constrained to be planar (AFIX 93 in SHELXL). C–H distances in CH_3 groups were constrained to 0.98 Å, those in CH_2 groups to 0.99 Å and those in CH groups to 1.00 Å. N–H distances in **1** and **2** were constrained to 0.88 Å. For compound **2**, reflection (562) strongly disagreed with the structural model and was therefore omitted from the refinement. In the case of compound **3**, one N-bonded methyl group (C11) was refined as rotationally disordered over two positions. Site occupancy factors were refined freely to 0.59 (2) for H12A, H13A and H14A, and to 0.41 (2) for H12B, H13B and H14B.

Acknowledgements

The material is based on work supported by the National Science Foundation under CHE-1461175. General financial support by the Otto-von-Guericke-Universität Magdeburg is also gratefully acknowledged.

References

- Agilent (2003). *CrysAlis PRO*. Agilent Technologies, Yarnton, England.
- Altomare, A., Burla, M. C., Camalli, M., Cascarano, G. L., Giacovazzo, C., Guagliardi, A., Moliterni, A. G. G., Polidori, G. & Spagna, R. (1999). *J. Appl. Cryst.* **32**, 115–119.
- Bassanetti, I., Atzeri, C., Tinonin, D. A. & Marchiò, L. (2016). *Cryst. Growth Des.* **16**, 3543–3552.
- Bernstein, J., Davis, R. E., Shimoni, L. & Chang, N.-L. (1995). *Angew. Chem. Int. Ed. Engl.* **34**, 1555–1573.
- Bigmore, H. R., Lawrence, S. C., Mountford, P. & Tredget, C. S. (2005). *Dalton Trans.* pp. 635–651.
- Brandenburg, K. (1999). *DIAMOND*. Crystal Impact GbR, Bonn, Germany.
- D'Amico, D. J., McDougal, M. A., Amenta, D. S., Gilje, J. W., Wang, S., Hrib, C. G. & Edelmann, F. T. (2015). *Polyhedron*, **88**, 19–28.
- Girma, K. B., Lorenz, V., Blaurock, S. & Edelmann, F. T. (2008). *Z. Anorg. Allg. Chem.* **634**, 267–273.
- Krieck, S., Koch, A., Hinze, K., Müller, C., Lange, J., Görls, H. & Westerhausen, M. (2016). *Eur. J. Inorg. Chem.* pp. 2332–2348.
- Marques, N., Sella, A. & Takats, J. (2002). *Chem. Rev.* **102**, 2137–2160.
- Mauret, P., Fayet, J. P., Fabre, M., Elguero, J. & De Mendoza, J. (1974). *J. Chim. Phys. Chim. Biol.* **71**, 115–116.
- McGaughey, G. B., Gagné, M. & Rappé, A. K. (1998). *J. Biol. Chem.* **273**, 15458–15463.
- Negri, F. & Caminati, W. (1996). *Chem. Phys. Lett.* **260**, 119–124.
- Nesmeyanov, A. N., Babin, V. N., Fedorov, L. A., Rybinskaya, M. I. & Fedin, E. I. (1969). *Tetrahedron*, **25**, 4667–4670.
- Otero, A., Fernández-Baeza, J., Lara-Sánchez, A. & Sánchez-Barba, L. F. (2013). *Coord. Chem. Rev.* **257**, 1806–1868.
- Paulo, A., Correia, J. D. G., Campello, M. P. C. & Santos, I. A. (2004). *Polyhedron*, **23**, 331–360.
- Poznański, J., Najda, A., Bretner, M. & Shugar, D. (2007). *J. Phys. Chem. A*, **111**, 6501–6509.
- Semeniuc, R. F. & Reger, D. L. (2016). *Eur. J. Inorg. Chem.* pp. 2253–2271.
- Sheldrick, G. M. (2008). *Acta Cryst. A* **64**, 112–122.
- Sheldrick, G. M. (2015). *Acta Cryst. C* **71**, 3–8.
- Smith, J. M. (2008). *Comments Inorg. Chem.* **29**, 189–233.
- Stoe & Cie (2002). *X-Area* and *X-RED*. Stoe & Cie, Darmstadt, Germany.
- Trofimenko, S. (1993). *Chem. Rev.* **93**, 943–980.
- Trofimenko, S. (2004). *Polyhedron*, **23**, 197–203.
- Wagner, T., Hrib, C. G., Lorenz, V., Edelmann, F. T., Zhang, J. & Li, Q. (2012). *Z. Anorg. Allg. Chem.* **638**, 2185–2188.
- Wang, S., Liebing, P., Oehler, F., Gilje, J. W., Hrib, C. G. & Edelmann, F. T. (2017). *Cryst. Growth Des.* **17** doi: 10.1021/acs.cgd.7b00361.

supporting information

Acta Cryst. (2017). E73, 880-885 [https://doi.org/10.1107/S2056989017007472]

Synthesis and crystal structures of three new benzotriazolylpropanamides

Donna S. Amenta, Phil Liebing, Julia E. Biero, Robert J. Sherman, John W. Gilje and Frank T. Edelmann

Computing details

Data collection: *CrysAlis PRO* (Agilent, 2003) for (1); *X-AREA* (Stoe & Cie, 2002) for (2), (3). Cell refinement: *CrysAlis PRO* (Agilent, 2003) for (1); *X-AREA* (Stoe & Cie, 2002) for (2), (3). Data reduction: *CrysAlis PRO* (Agilent, 2003) for (1); *X-AREA* and *X-RED* (Stoe & Cie, 2002) for (2), (3). Program(s) used to solve structure: *SHELXS97* (Sheldrick, 2008) for (1), (2); *SIR97* (Altomare *et al.*, 1999) for (3). For all compounds, program(s) used to refine structure: *SHELXL2016* (Sheldrick, 2015); molecular graphics: *DIAMOND* (Brandenburg, 1999); software used to prepare material for publication: *SHELXL2016* (Sheldrick, 2015).

(1) 3-(1*H*-Benzotriazol-1-yl)-2-methylpropanamide

Crystal data

$C_{10}H_{12}N_4O$
 $M_r = 204.24$
Triclinic, $P\bar{1}$
 $a = 7.3885$ (9) Å
 $b = 8.072$ (1) Å
 $c = 9.2976$ (13) Å
 $\alpha = 69.039$ (12)°
 $\beta = 89.498$ (10)°
 $\gamma = 75.915$ (10)°
 $V = 500.37$ (12) Å³

$Z = 2$
 $F(000) = 216$
 $D_x = 1.356$ Mg m⁻³
Cu $K\alpha$ radiation, $\lambda = 1.54184$ Å
Cell parameters from 21215 reflections
 $\theta = 5.1\text{--}76.1^\circ$
 $\mu = 0.76$ mm⁻¹
 $T = 100$ K
Prism, colorless
0.15 × 0.10 × 0.08 mm

Data collection

Agilent Xcalibur, Atlas, Nova
diffractometer
Radiation source: fine-focus sealed tube
Detector resolution: 10.3543 pixels mm⁻¹
 ω scans
Absorption correction: multi-scan
(CrysAlis PRO, Agilent, 2003)
 $T_{\min} = 0.919$, $T_{\max} = 1.000$

28193 measured reflections
2053 independent reflections
2012 reflections with $I > 2\sigma(I)$
 $R_{\text{int}} = 0.026$
 $\theta_{\max} = 75.0^\circ$, $\theta_{\min} = 5.1^\circ$
 $h = -9 \rightarrow 9$
 $k = -10 \rightarrow 10$
 $l = -9 \rightarrow 11$

Refinement

Refinement on F^2
Least-squares matrix: full
 $R[F^2 > 2\sigma(F^2)] = 0.032$
 $wR(F^2) = 0.081$
 $S = 1.11$
2053 reflections

138 parameters
0 restraints
Primary atom site location: structure-invariant
direct methods
Secondary atom site location: difference Fourier
map

Hydrogen site location: inferred from neighbouring sites

H-atom parameters constrained

$$w = 1/[\sigma^2(F_o^2) + (0.0349P)^2 + 0.1806P]$$

$$\text{where } P = (F_o^2 + 2F_c^2)/3$$

$$(\Delta/\sigma)_{\max} < 0.001$$

$$\Delta\rho_{\max} = 0.33 \text{ e } \text{\AA}^{-3}$$

$$\Delta\rho_{\min} = -0.21 \text{ e } \text{\AA}^{-3}$$

Extinction correction: SHELXL2016

(Sheldrick, 2015),

$$Fc^* = kFc[1 + 0.001xFc^2\lambda^3/\sin(2\theta)]^{-1/4}$$

Extinction coefficient: 0.0117 (12)

Special details

Geometry. All esds (except the esd in the dihedral angle between two l.s. planes) are estimated using the full covariance matrix. The cell esds are taken into account individually in the estimation of esds in distances, angles and torsion angles; correlations between esds in cell parameters are only used when they are defined by crystal symmetry. An approximate (isotropic) treatment of cell esds is used for estimating esds involving l.s. planes.

Fractional atomic coordinates and isotropic or equivalent isotropic displacement parameters (\AA^2)

	<i>x</i>	<i>y</i>	<i>z</i>	$U_{\text{iso}}^*/U_{\text{eq}}$
C1	0.15133 (14)	0.68751 (14)	0.89673 (11)	0.0176 (2)
C2	0.25594 (14)	0.83380 (13)	0.82012 (11)	0.0179 (2)
H3	0.165006	0.949315	0.752342	0.022*
C3	0.40506 (14)	0.76911 (14)	0.72364 (11)	0.0184 (2)
H4	0.488091	0.853320	0.694399	0.022*
H5	0.482564	0.645326	0.787098	0.022*
C4	0.35221 (17)	0.87131 (16)	0.94623 (13)	0.0262 (3)
H8	0.258168	0.911025	1.010223	0.031*
H6	0.416372	0.967988	0.898144	0.031*
H7	0.443677	0.758907	1.011003	0.031*
C5	0.29153 (13)	0.61763 (14)	0.55521 (12)	0.0167 (2)
C6	0.21574 (14)	0.69407 (14)	0.40143 (12)	0.0181 (2)
C7	0.16602 (14)	0.58415 (15)	0.32859 (12)	0.0213 (2)
H9	0.113426	0.634772	0.224400	0.026*
C8	0.19688 (14)	0.40025 (15)	0.41480 (13)	0.0220 (2)
H10	0.165146	0.321802	0.369143	0.026*
C9	0.27490 (14)	0.32485 (14)	0.57016 (13)	0.0214 (2)
H11	0.294873	0.196704	0.625394	0.026*
C10	0.32283 (14)	0.43018 (14)	0.64405 (12)	0.0191 (2)
H12	0.373910	0.379176	0.748680	0.023*
N1	-0.03436 (12)	0.74707 (12)	0.89024 (10)	0.0209 (2)
H2	-0.101453	0.669647	0.936062	0.025*
H1	-0.089861	0.863817	0.840137	0.025*
N2	0.32450 (12)	0.76231 (11)	0.58395 (10)	0.0173 (2)
N3	0.27302 (13)	0.91737 (12)	0.45699 (10)	0.0209 (2)
N4	0.20701 (13)	0.87851 (12)	0.34604 (10)	0.0213 (2)
O	0.23854 (10)	0.52560 (10)	0.96498 (9)	0.02255 (19)

Atomic displacement parameters (\AA^2)

	U^{11}	U^{22}	U^{33}	U^{12}	U^{13}	U^{23}
C1	0.0225 (5)	0.0179 (5)	0.0130 (4)	-0.0063 (4)	0.0019 (4)	-0.0056 (4)
C2	0.0214 (5)	0.0164 (5)	0.0158 (5)	-0.0061 (4)	0.0012 (4)	-0.0049 (4)

C3	0.0195 (5)	0.0197 (5)	0.0171 (5)	-0.0071 (4)	0.0007 (4)	-0.0065 (4)
C4	0.0344 (6)	0.0286 (6)	0.0207 (5)	-0.0144 (5)	0.0023 (4)	-0.0110 (4)
C5	0.0152 (4)	0.0180 (5)	0.0173 (5)	-0.0046 (4)	0.0030 (4)	-0.0068 (4)
C6	0.0171 (5)	0.0187 (5)	0.0163 (5)	-0.0030 (4)	0.0026 (4)	-0.0048 (4)
C7	0.0190 (5)	0.0278 (6)	0.0182 (5)	-0.0050 (4)	0.0021 (4)	-0.0103 (4)
C8	0.0200 (5)	0.0259 (5)	0.0258 (6)	-0.0083 (4)	0.0055 (4)	-0.0148 (4)
C9	0.0209 (5)	0.0178 (5)	0.0256 (5)	-0.0063 (4)	0.0053 (4)	-0.0071 (4)
C10	0.0187 (5)	0.0182 (5)	0.0178 (5)	-0.0049 (4)	0.0021 (4)	-0.0035 (4)
N1	0.0207 (4)	0.0165 (4)	0.0213 (4)	-0.0050 (3)	0.0022 (3)	-0.0018 (3)
N2	0.0206 (4)	0.0152 (4)	0.0148 (4)	-0.0053 (3)	0.0018 (3)	-0.0037 (3)
N3	0.0255 (5)	0.0170 (4)	0.0170 (4)	-0.0046 (3)	0.0022 (3)	-0.0032 (3)
N4	0.0247 (5)	0.0195 (4)	0.0170 (4)	-0.0037 (4)	0.0007 (3)	-0.0050 (3)
O	0.0222 (4)	0.0172 (4)	0.0234 (4)	-0.0045 (3)	0.0025 (3)	-0.0020 (3)

Geometric parameters (\AA , $^{\circ}$)

C1—O	1.2369 (13)	C5—C10	1.4014 (14)
C1—N1	1.3329 (14)	C6—N4	1.3752 (13)
C1—C2	1.5271 (14)	C6—C7	1.4049 (15)
C2—C3	1.5261 (14)	C7—C8	1.3730 (15)
C2—C4	1.5316 (14)	C7—H9	0.9500
C2—H3	1.0000	C8—C9	1.4157 (16)
C3—N2	1.4576 (13)	C8—H10	0.9500
C3—H4	0.9900	C9—C10	1.3744 (15)
C3—H5	0.9900	C9—H11	0.9500
C4—H8	0.9800	C10—H12	0.9500
C4—H6	0.9800	N1—H2	0.8800
C4—H7	0.9800	N1—H1	0.8800
C5—N2	1.3628 (13)	N2—N3	1.3505 (12)
C5—C6	1.3977 (14)	N3—N4	1.3096 (13)
O—C1—N1	123.48 (9)	N4—C6—C5	108.40 (9)
O—C1—C2	120.43 (9)	N4—C6—C7	130.82 (10)
N1—C1—C2	116.03 (9)	C5—C6—C7	120.77 (10)
C3—C2—C1	110.96 (8)	C8—C7—C6	116.99 (10)
C3—C2—C4	108.61 (9)	C8—C7—H9	121.5
C1—C2—C4	108.83 (8)	C6—C7—H9	121.5
C3—C2—H3	109.5	C7—C8—C9	121.51 (10)
C1—C2—H3	109.5	C7—C8—H10	119.2
C4—C2—H3	109.5	C9—C8—H10	119.2
N2—C3—C2	112.50 (8)	C10—C9—C8	122.44 (10)
N2—C3—H4	109.1	C10—C9—H11	118.8
C2—C3—H4	109.1	C8—C9—H11	118.8
N2—C3—H5	109.1	C9—C10—C5	115.74 (10)
C2—C3—H5	109.1	C9—C10—H12	122.1
H4—C3—H5	107.8	C5—C10—H12	122.1
C2—C4—H8	109.5	C1—N1—H2	120.0
C2—C4—H6	109.5	C1—N1—H1	120.0

H8—C4—H6	109.5	H2—N1—H1	120.0
C2—C4—H7	109.5	N3—N2—C5	110.44 (8)
H8—C4—H7	109.5	N3—N2—C3	119.41 (8)
H6—C4—H7	109.5	C5—N2—C3	130.14 (8)
N2—C5—C6	104.07 (9)	N4—N3—N2	108.81 (8)
N2—C5—C10	133.36 (9)	N3—N4—C6	108.28 (8)
C6—C5—C10	122.55 (10)		
O—C1—C2—C3	47.10 (12)	C8—C9—C10—C5	-0.69 (15)
N1—C1—C2—C3	-135.56 (9)	N2—C5—C10—C9	-177.82 (10)
O—C1—C2—C4	-72.35 (12)	C6—C5—C10—C9	0.27 (15)
N1—C1—C2—C4	104.99 (10)	C6—C5—N2—N3	-0.07 (11)
C1—C2—C3—N2	70.99 (10)	C10—C5—N2—N3	178.28 (11)
C4—C2—C3—N2	-169.42 (8)	C6—C5—N2—C3	-179.08 (9)
N2—C5—C6—N4	0.01 (11)	C10—C5—N2—C3	-0.74 (18)
C10—C5—C6—N4	-178.56 (9)	C2—C3—N2—N3	82.84 (11)
N2—C5—C6—C7	178.91 (9)	C2—C3—N2—C5	-98.22 (12)
C10—C5—C6—C7	0.34 (15)	C5—N2—N3—N4	0.11 (11)
N4—C6—C7—C8	178.10 (10)	C3—N2—N3—N4	179.24 (8)
C5—C6—C7—C8	-0.53 (15)	N2—N3—N4—C6	-0.10 (11)
C6—C7—C8—C9	0.13 (15)	C5—C6—N4—N3	0.06 (11)
C7—C8—C9—C10	0.51 (16)	C7—C6—N4—N3	-178.70 (10)

Hydrogen-bond geometry (Å, °)

D—H···A	D—H	H···A	D···A	D—H···A
N1—H2···O ⁱ	0.88	2.02	2.8970 (12)	175
N1—H1···N4 ⁱⁱ	0.88	2.16	3.0017 (14)	161

Symmetry codes: (i) $-x, -y+1, -z+2$; (ii) $-x, -y+2, -z+1$.(2) 3-(2*H*-Benzotriazol-2-yl)-2-methylpropanamide*Crystal data*

$\text{C}_{10}\text{H}_{12}\text{N}_4\text{O}$	$Z = 2$
$M_r = 204.24$	$F(000) = 216$
Triclinic, $P\bar{1}$	$D_x = 1.329 \text{ Mg m}^{-3}$
$a = 5.5961 (11) \text{ \AA}$	Mo $K\alpha$ radiation, $\lambda = 0.71073 \text{ \AA}$
$b = 9.3462 (19) \text{ \AA}$	Cell parameters from 5587 reflections
$c = 10.472 (2) \text{ \AA}$	$\theta = 2.1\text{--}29.2^\circ$
$\alpha = 109.83 (3)^\circ$	$\mu = 0.09 \text{ mm}^{-1}$
$\beta = 90.93 (3)^\circ$	$T = 133 \text{ K}$
$\gamma = 97.14 (3)^\circ$	Prism, colorless
$V = 510.2 (2) \text{ \AA}^3$	$0.48 \times 0.33 \times 0.25 \text{ mm}$

Data collection

Stoe IPDS 2T diffractometer	3731 measured reflections 1774 independent reflections
Radiation source: fine-focus sealed tube	1653 reflections with $I > 2\sigma(I)$
Detector resolution: 6.67 pixels mm^{-1} area detector scans	$R_{\text{int}} = 0.056$ $\theta_{\text{max}} = 25.0^\circ, \theta_{\text{min}} = 2.1^\circ$

$h = -6 \rightarrow 6$
 $k = -11 \rightarrow 11$

$l = -12 \rightarrow 12$

Refinement

Refinement on F^2
 Least-squares matrix: full
 $R[F^2 > 2\sigma(F^2)] = 0.037$
 $wR(F^2) = 0.087$
 $S = 1.09$
 1774 reflections
 138 parameters
 0 restraints
 Primary atom site location: structure-invariant direct methods
 Secondary atom site location: difference Fourier map

Hydrogen site location: inferred from neighbouring sites
 H-atom parameters constrained
 $w = 1/[\sigma^2(F_o^2) + (0.028P)^2 + 0.190P]$
 where $P = (F_o^2 + 2F_c^2)/3$
 $(\Delta/\sigma)_{\text{max}} < 0.001$
 $\Delta\rho_{\text{max}} = 0.25 \text{ e } \text{\AA}^{-3}$
 $\Delta\rho_{\text{min}} = -0.18 \text{ e } \text{\AA}^{-3}$
 Extinction correction: SHELXL2016 (Sheldrick, 2015),
 $F_c^* = kFc[1 + 0.001xFc^2\lambda^3/\sin(2\theta)]^{-1/4}$
 Extinction coefficient: 0.11 (2)

Special details

Geometry. All esds (except the esd in the dihedral angle between two l.s. planes) are estimated using the full covariance matrix. The cell esds are taken into account individually in the estimation of esds in distances, angles and torsion angles; correlations between esds in cell parameters are only used when they are defined by crystal symmetry. An approximate (isotropic) treatment of cell esds is used for estimating esds involving l.s. planes.

Fractional atomic coordinates and isotropic or equivalent isotropic displacement parameters (\AA^2)

	x	y	z	$U_{\text{iso}}^*/U_{\text{eq}}$
C1	0.0227 (2)	0.64543 (13)	0.69653 (13)	0.0214 (3)
C2	0.0204 (2)	0.74112 (14)	0.84610 (13)	0.0225 (3)
H3	-0.098923	0.815190	0.857903	0.027*
C3	0.2682 (3)	0.82849 (15)	0.90085 (13)	0.0252 (3)
H5	0.262252	0.888303	0.998666	0.030*
H4	0.383837	0.754250	0.892496	0.030*
C4	-0.0516 (3)	0.63442 (17)	0.92572 (15)	0.0341 (4)
H6	-0.215805	0.581749	0.895255	0.041*
H8	-0.045568	0.694636	1.022969	0.041*
H7	0.060441	0.558341	0.910078	0.041*
C5	0.5730 (2)	1.03192 (15)	0.71230 (13)	0.0223 (3)
C6	0.3863 (2)	1.11949 (15)	0.75999 (13)	0.0232 (3)
C7	0.3662 (3)	1.25214 (16)	0.72735 (15)	0.0298 (3)
H9	0.239683	1.311962	0.758654	0.036*
C8	0.5363 (3)	1.29041 (17)	0.64894 (15)	0.0325 (4)
H10	0.528050	1.379345	0.625352	0.039*
C9	0.7253 (3)	1.20216 (18)	0.60133 (15)	0.0347 (4)
H11	0.840016	1.233870	0.547020	0.042*
C10	0.7479 (3)	1.07309 (17)	0.63095 (15)	0.0311 (4)
H12	0.874723	1.014003	0.598479	0.037*
N1	-0.1609 (2)	0.64790 (12)	0.61694 (11)	0.0250 (3)
H1	-0.170803	0.591949	0.529944	0.030*
H2	-0.273477	0.705494	0.650863	0.030*
N2	0.5490 (2)	0.91227 (12)	0.75780 (11)	0.0239 (3)

N3	0.3548 (2)	0.93272 (12)	0.82946 (11)	0.0220 (3)
N4	0.2480 (2)	1.05296 (13)	0.83583 (12)	0.0258 (3)
O	0.18732 (19)	0.56749 (11)	0.65622 (10)	0.0320 (3)

Atomic displacement parameters (\AA^2)

	U^{11}	U^{22}	U^{33}	U^{12}	U^{13}	U^{23}
C1	0.0270 (7)	0.0161 (6)	0.0212 (7)	0.0033 (5)	0.0079 (5)	0.0062 (5)
C2	0.0281 (7)	0.0205 (6)	0.0194 (7)	0.0058 (5)	0.0064 (5)	0.0065 (5)
C3	0.0304 (7)	0.0262 (7)	0.0195 (6)	0.0050 (6)	0.0012 (5)	0.0084 (5)
C4	0.0497 (10)	0.0282 (7)	0.0268 (7)	0.0063 (7)	0.0146 (7)	0.0116 (6)
C5	0.0203 (7)	0.0247 (6)	0.0197 (6)	0.0020 (5)	-0.0010 (5)	0.0053 (5)
C6	0.0207 (7)	0.0240 (6)	0.0221 (7)	0.0005 (5)	0.0007 (5)	0.0050 (5)
C7	0.0279 (8)	0.0265 (7)	0.0351 (8)	0.0044 (6)	0.0017 (6)	0.0104 (6)
C8	0.0330 (8)	0.0294 (7)	0.0361 (8)	-0.0040 (6)	-0.0060 (6)	0.0157 (6)
C9	0.0273 (8)	0.0466 (9)	0.0323 (8)	-0.0058 (7)	0.0017 (6)	0.0198 (7)
C10	0.0230 (7)	0.0412 (8)	0.0296 (7)	0.0047 (6)	0.0062 (6)	0.0124 (6)
N1	0.0286 (6)	0.0252 (6)	0.0203 (6)	0.0096 (5)	0.0050 (5)	0.0042 (4)
N2	0.0226 (6)	0.0267 (6)	0.0210 (6)	0.0050 (5)	0.0029 (4)	0.0057 (4)
N3	0.0230 (6)	0.0212 (5)	0.0203 (6)	0.0029 (4)	0.0010 (4)	0.0051 (4)
N4	0.0250 (6)	0.0246 (6)	0.0276 (6)	0.0045 (5)	0.0050 (5)	0.0080 (5)
O	0.0331 (6)	0.0341 (6)	0.0240 (5)	0.0136 (5)	0.0027 (4)	0.0008 (4)

Geometric parameters (\AA , $^\circ$)

C1—O	1.2364 (16)	C5—C10	1.410 (2)
C1—N1	1.3199 (18)	C6—N4	1.3607 (18)
C1—C2	1.5187 (18)	C6—C7	1.4098 (19)
C2—C3	1.514 (2)	C7—C8	1.360 (2)
C2—C4	1.5255 (18)	C7—H9	0.9500
C2—H3	1.0000	C8—C9	1.415 (2)
C3—N3	1.4598 (17)	C8—H10	0.9500
C3—H5	0.9900	C9—C10	1.363 (2)
C3—H4	0.9900	C9—H11	0.9500
C4—H6	0.9800	C10—H12	0.9500
C4—H8	0.9800	N1—H1	0.8800
C4—H7	0.9800	N1—H2	0.8800
C5—N2	1.3498 (18)	N2—N3	1.3276 (16)
C5—C6	1.4013 (19)	N3—N4	1.3198 (16)
O—C1—N1	123.67 (12)	N4—C6—C5	108.31 (12)
O—C1—C2	119.91 (12)	N4—C6—C7	130.81 (13)
N1—C1—C2	116.40 (11)	C5—C6—C7	120.88 (13)
C3—C2—C1	110.76 (11)	C8—C7—C6	116.86 (13)
C3—C2—C4	108.52 (12)	C8—C7—H9	121.6
C1—C2—C4	108.88 (11)	C6—C7—H9	121.6
C3—C2—H3	109.6	C7—C8—C9	122.17 (13)
C1—C2—H3	109.6	C7—C8—H10	118.9

C4—C2—H3	109.6	C9—C8—H10	118.9
N3—C3—C2	112.65 (11)	C10—C9—C8	122.07 (14)
N3—C3—H5	109.1	C10—C9—H11	119.0
C2—C3—H5	109.1	C8—C9—H11	119.0
N3—C3—H4	109.1	C9—C10—C5	116.47 (14)
C2—C3—H4	109.1	C9—C10—H12	121.8
H5—C3—H4	107.8	C5—C10—H12	121.8
C2—C4—H6	109.5	C1—N1—H1	120.0
C2—C4—H8	109.5	C1—N1—H2	120.0
H6—C4—H8	109.5	H1—N1—H2	120.0
C2—C4—H7	109.5	N3—N2—C5	103.09 (11)
H6—C4—H7	109.5	N4—N3—N2	117.11 (11)
H8—C4—H7	109.5	N4—N3—C3	121.80 (11)
N2—C5—C6	108.57 (12)	N2—N3—C3	121.07 (11)
N2—C5—C10	129.88 (13)	N3—N4—C6	102.93 (11)
C6—C5—C10	121.56 (13)		
O—C1—C2—C3	45.53 (16)	C8—C9—C10—C5	-0.2 (2)
N1—C1—C2—C3	-136.47 (12)	N2—C5—C10—C9	-179.87 (13)
O—C1—C2—C4	-73.73 (16)	C6—C5—C10—C9	0.0 (2)
N1—C1—C2—C4	104.27 (14)	C6—C5—N2—N3	-0.24 (13)
C1—C2—C3—N3	59.74 (14)	C10—C5—N2—N3	179.62 (14)
C4—C2—C3—N3	179.22 (10)	C5—N2—N3—N4	0.10 (14)
N2—C5—C6—N4	0.30 (14)	C5—N2—N3—C3	-178.27 (11)
C10—C5—C6—N4	-179.57 (12)	C2—C3—N3—N4	65.73 (15)
N2—C5—C6—C7	-179.77 (12)	C2—C3—N3—N2	-115.97 (13)
C10—C5—C6—C7	0.4 (2)	N2—N3—N4—C6	0.08 (15)
N4—C6—C7—C8	179.50 (14)	C3—N3—N4—C6	178.44 (11)
C5—C6—C7—C8	-0.41 (19)	C5—C6—N4—N3	-0.23 (14)
C6—C7—C8—C9	0.2 (2)	C7—C6—N4—N3	179.86 (13)
C7—C8—C9—C10	0.2 (2)		

Hydrogen-bond geometry (Å, °)

D—H···A	D—H	H···A	D···A	D—H···A
N1—H1···O ⁱ	0.88	2.00	2.8745 (18)	170
N1—H2···N2 ⁱⁱ	0.88	2.24	3.0850 (18)	161

Symmetry codes: (i) $-x, -y+1, -z+1$; (ii) $x-1, y, z$.(3) 3-(1*H*-Benzotriazol-1-yl)-*N,N*-dimethylpropanamide*Crystal data*

C ₁₁ H ₁₄ N ₄ O	$\beta = 86.247 (6)^\circ$
$M_r = 218.26$	$\gamma = 81.528 (6)^\circ$
Triclinic, $P\bar{1}$	$V = 540.25 (7) \text{ \AA}^3$
$a = 7.1732 (6) \text{ \AA}$	$Z = 2$
$b = 7.9945 (6) \text{ \AA}$	$F(000) = 232$
$c = 9.5912 (7) \text{ \AA}$	$D_x = 1.342 \text{ Mg m}^{-3}$
$\alpha = 83.910 (6)^\circ$	Mo $K\alpha$ radiation, $\lambda = 0.71073 \text{ \AA}$

Cell parameters from 6240 reflections
 $\theta = 2.1\text{--}29.2^\circ$
 $\mu = 0.09 \text{ mm}^{-1}$

$T = 153 \text{ K}$
Block, colorless
 $0.34 \times 0.32 \times 0.28 \text{ mm}$

Data collection

Stoe IPDS 2T
diffractometer
Radiation source: fine-focus sealed tube
Detector resolution: 6.67 pixels mm^{-1}
area detector scans
4194 measured reflections
1904 independent reflections

1596 reflections with $I > 2\sigma(I)$
 $R_{\text{int}} = 0.062$
 $\theta_{\text{max}} = 25.0^\circ, \theta_{\text{min}} = 2.1^\circ$
 $h = -8 \rightarrow 8$
 $k = -9 \rightarrow 9$
 $l = -11 \rightarrow 11$

Refinement

Refinement on F^2
Least-squares matrix: full
 $R[F^2 > 2\sigma(F^2)] = 0.047$
 $wR(F^2) = 0.131$
 $S = 1.03$
1904 reflections
149 parameters
0 restraints
Primary atom site location: structure-invariant
direct methods
Secondary atom site location: difference Fourier
map

Hydrogen site location: inferred from
neighbouring sites
H-atom parameters constrained
 $w = 1/[\sigma^2(F_o^2) + (0.0794P)^2 + 0.073P]$
where $P = (F_o^2 + 2F_c^2)/3$
 $(\Delta/\sigma)_{\text{max}} = 0.001$
 $\Delta\rho_{\text{max}} = 0.22 \text{ e } \text{\AA}^{-3}$
 $\Delta\rho_{\text{min}} = -0.20 \text{ e } \text{\AA}^{-3}$
Extinction correction: SHELXL2016
(Sheldrick, 2015),
 $F_c^* = kF_c[1 + 0.001xF_c^2\lambda^3/\sin(2\theta)]^{-1/4}$
Extinction coefficient: 0.062 (15)

Special details

Geometry. All esds (except the esd in the dihedral angle between two l.s. planes) are estimated using the full covariance matrix. The cell esds are taken into account individually in the estimation of esds in distances, angles and torsion angles; correlations between esds in cell parameters are only used when they are defined by crystal symmetry. An approximate (isotropic) treatment of cell esds is used for estimating esds involving l.s. planes.

Fractional atomic coordinates and isotropic or equivalent isotropic displacement parameters (\AA^2)

	x	y	z	$U_{\text{iso}}^*/U_{\text{eq}}$	Occ. (<1)
C1	0.2374 (2)	0.1609 (2)	0.89843 (17)	0.0317 (4)	
C2	0.2225 (3)	0.3473 (2)	0.91977 (18)	0.0357 (4)	
H2	0.312766	0.361341	0.990012	0.043*	
H1	0.093801	0.387131	0.957760	0.043*	
C3	0.2629 (3)	0.4566 (2)	0.78541 (18)	0.0363 (4)	
H4	0.187972	0.427798	0.710496	0.044*	
H3	0.221528	0.577397	0.800163	0.044*	
C4	0.5548 (2)	0.34481 (19)	0.63744 (16)	0.0308 (4)	
C5	0.7407 (3)	0.3710 (2)	0.64288 (17)	0.0356 (4)	
C6	0.8817 (3)	0.2937 (2)	0.5534 (2)	0.0441 (5)	
H5	1.009954	0.309393	0.557083	0.053*	
C7	0.8268 (3)	0.1947 (2)	0.46046 (19)	0.0441 (5)	
H6	0.919384	0.139249	0.398995	0.053*	
C8	0.6372 (3)	0.1724 (2)	0.45317 (18)	0.0397 (5)	
H7	0.604940	0.104362	0.385487	0.048*	
C9	0.4981 (3)	0.2455 (2)	0.54036 (17)	0.0352 (4)	

H8	0.370003	0.230034	0.535556	0.042*	
C10	0.2411 (3)	0.0869 (3)	1.15684 (19)	0.0505 (5)	
H10	0.138000	0.036749	1.209814	0.061*	
H9	0.219291	0.210450	1.159458	0.061*	
H11	0.360994	0.040258	1.198882	0.061*	
C11	0.2605 (3)	-0.1321 (2)	0.9926 (2)	0.0454 (5)	
H13A	0.386119	-0.190604	1.015826	0.054*	0.59 (2)
H14A	0.238741	-0.144173	0.894596	0.054*	0.59 (2)
H12A	0.164666	-0.182399	1.054197	0.054*	0.59 (2)
H12B	0.140231	-0.154180	0.960587	0.054*	0.41 (2)
H13B	0.287609	-0.200611	1.081816	0.054*	0.41 (2)
H14B	0.361685	-0.162385	0.922216	0.054*	0.41 (2)
N1	0.2484 (2)	0.04712 (18)	1.01231 (15)	0.0362 (4)	
N2	0.4605 (2)	0.43518 (16)	0.73920 (14)	0.0327 (4)	
N3	0.5824 (2)	0.51402 (18)	0.80163 (15)	0.0390 (4)	
N4	0.7510 (2)	0.4768 (2)	0.74587 (16)	0.0422 (4)	
O	0.2366 (2)	0.11687 (15)	0.77971 (13)	0.0442 (4)	

Atomic displacement parameters (\AA^2)

	U^{11}	U^{22}	U^{33}	U^{12}	U^{13}	U^{23}
C1	0.0305 (8)	0.0308 (8)	0.0359 (9)	-0.0073 (6)	-0.0002 (7)	-0.0095 (7)
C2	0.0391 (10)	0.0295 (8)	0.0404 (9)	-0.0059 (7)	0.0002 (7)	-0.0114 (7)
C3	0.0403 (10)	0.0251 (8)	0.0446 (9)	-0.0027 (7)	-0.0055 (8)	-0.0088 (7)
C4	0.0403 (9)	0.0226 (7)	0.0307 (8)	-0.0074 (7)	-0.0052 (7)	-0.0021 (6)
C5	0.0421 (10)	0.0325 (8)	0.0345 (8)	-0.0118 (7)	-0.0058 (7)	-0.0020 (7)
C6	0.0380 (10)	0.0498 (11)	0.0452 (10)	-0.0101 (8)	-0.0022 (8)	-0.0020 (8)
C7	0.0528 (12)	0.0388 (10)	0.0387 (10)	-0.0024 (8)	0.0040 (8)	-0.0046 (7)
C8	0.0592 (12)	0.0289 (8)	0.0330 (9)	-0.0102 (8)	-0.0031 (8)	-0.0066 (7)
C9	0.0453 (10)	0.0281 (8)	0.0352 (9)	-0.0111 (7)	-0.0066 (7)	-0.0064 (7)
C10	0.0641 (13)	0.0521 (12)	0.0382 (10)	-0.0184 (10)	-0.0010 (9)	-0.0050 (8)
C11	0.0473 (11)	0.0292 (9)	0.0601 (12)	-0.0079 (8)	-0.0025 (9)	-0.0032 (8)
N1	0.0405 (8)	0.0313 (7)	0.0386 (8)	-0.0088 (6)	-0.0016 (6)	-0.0065 (6)
N2	0.0418 (8)	0.0245 (6)	0.0349 (7)	-0.0102 (6)	-0.0056 (6)	-0.0071 (5)
N3	0.0482 (9)	0.0340 (7)	0.0401 (8)	-0.0164 (7)	-0.0093 (7)	-0.0090 (6)
N4	0.0446 (9)	0.0438 (9)	0.0429 (8)	-0.0166 (7)	-0.0073 (7)	-0.0092 (7)
O	0.0648 (9)	0.0330 (7)	0.0382 (7)	-0.0126 (6)	-0.0033 (6)	-0.0111 (5)

Geometric parameters (\AA , $^\circ$)

C1—O	1.228 (2)	C7—H6	0.9500
C1—N1	1.344 (2)	C8—C9	1.364 (3)
C1—C2	1.513 (2)	C8—H7	0.9500
C2—C3	1.515 (2)	C9—H8	0.9500
C2—H2	0.9900	C10—N1	1.451 (2)
C2—H1	0.9900	C10—H10	0.9800
C3—N2	1.448 (2)	C10—H9	0.9800
C3—H4	0.9900	C10—H11	0.9800

C3—H3	0.9900	C11—N1	1.455 (2)
C4—N2	1.361 (2)	C11—H13A	0.9800
C4—C5	1.385 (3)	C11—H14A	0.9800
C4—C9	1.401 (2)	C11—H12A	0.9800
C5—N4	1.379 (2)	C11—H12B	0.9800
C5—C6	1.399 (3)	C11—H13B	0.9800
C6—C7	1.365 (3)	C11—H14B	0.9800
C6—H5	0.9500	N2—N3	1.3535 (19)
C7—C8	1.404 (3)	N3—N4	1.296 (2)
O—C1—N1	121.60 (14)	N1—C10—H9	109.5
O—C1—C2	120.14 (15)	H10—C10—H9	109.5
N1—C1—C2	118.25 (14)	N1—C10—H11	109.5
C1—C2—C3	112.71 (13)	H10—C10—H11	109.5
C1—C2—H2	109.1	H9—C10—H11	109.5
C3—C2—H2	109.1	N1—C11—H13A	109.5
C1—C2—H1	109.1	N1—C11—H14A	109.5
C3—C2—H1	109.1	H13A—C11—H14A	109.5
H2—C2—H1	107.8	N1—C11—H12A	109.5
N2—C3—C2	113.14 (14)	H13A—C11—H12A	109.5
N2—C3—H4	109.0	H14A—C11—H12A	109.5
C2—C3—H4	109.0	N1—C11—H12B	109.5
N2—C3—H3	109.0	H13A—C11—H12B	141.1
C2—C3—H3	109.0	H14A—C11—H12B	56.3
H4—C3—H3	107.8	H12A—C11—H12B	56.3
N2—C4—C5	104.46 (14)	N1—C11—H13B	109.5
N2—C4—C9	133.38 (16)	H13A—C11—H13B	56.3
C5—C4—C9	122.15 (16)	H14A—C11—H13B	141.1
N4—C5—C4	108.56 (16)	H12A—C11—H13B	56.3
N4—C5—C6	130.69 (17)	H12B—C11—H13B	109.5
C4—C5—C6	120.75 (16)	N1—C11—H14B	109.5
C7—C6—C5	117.01 (17)	H13A—C11—H14B	56.3
C7—C6—H5	121.5	H14A—C11—H14B	56.3
C5—C6—H5	121.5	H12A—C11—H14B	141.1
C6—C7—C8	121.86 (18)	H12B—C11—H14B	109.5
C6—C7—H6	119.1	H13B—C11—H14B	109.5
C8—C7—H6	119.1	C1—N1—C10	125.72 (14)
C9—C8—C7	121.95 (16)	C1—N1—C11	118.52 (14)
C9—C8—H7	119.0	C10—N1—C11	115.70 (15)
C7—C8—H7	119.0	N3—N2—C4	109.63 (14)
C8—C9—C4	116.25 (16)	N3—N2—C3	119.52 (13)
C8—C9—H8	121.9	C4—N2—C3	130.85 (14)
C4—C9—H8	121.9	N4—N3—N2	109.52 (13)
N1—C10—H10	109.5	N3—N4—C5	107.81 (14)
O—C1—C2—C3	-16.2 (2)	C2—C1—N1—C10	2.2 (3)
N1—C1—C2—C3	164.77 (15)	O—C1—N1—C11	0.2 (3)
C1—C2—C3—N2	-72.24 (18)	C2—C1—N1—C11	179.27 (15)

N2—C4—C5—N4	−0.66 (18)	C5—C4—N2—N3	0.86 (18)
C9—C4—C5—N4	178.42 (14)	C9—C4—N2—N3	−178.07 (17)
N2—C4—C5—C6	178.83 (15)	C5—C4—N2—C3	−179.29 (15)
C9—C4—C5—C6	−2.1 (3)	C9—C4—N2—C3	1.8 (3)
N4—C5—C6—C7	−179.73 (18)	C2—C3—N2—N3	−78.81 (17)
C4—C5—C6—C7	0.9 (3)	C2—C3—N2—C4	101.35 (19)
C5—C6—C7—C8	0.8 (3)	C4—N2—N3—N4	−0.77 (19)
C6—C7—C8—C9	−1.4 (3)	C3—N2—N3—N4	179.36 (14)
C7—C8—C9—C4	0.2 (2)	N2—N3—N4—C5	0.32 (18)
N2—C4—C9—C8	−179.75 (17)	C4—C5—N4—N3	0.23 (19)
C5—C4—C9—C8	1.5 (2)	C6—C5—N4—N3	−179.20 (18)
O—C1—N1—C10	−176.82 (17)		